A new structural element containing glycine-rich proteins and rhamnogalacturonan I in the protoxylem of seed plants

Ulrich Ryser[1],*, Martine Schorderet[1], Romain Guyot[2] and Beat Keller[2]

[1]University of Fribourg, Biology Department, Plant Biology, Fribourg, Switzerland
[2]University of Zürich, Institute of Plant Biology, Zürich Switzerland
*Author for correspondence (e-mail: ulrich.ryser@unifr.ch)

Summary

The water pipes of elongating plant organs are the result of programmed cell death and are formed by the walls of dead and empty protoxylem elements. These protoxylem elements are passively elongated many times by the surrounding tissue before they are replaced and collapse. Well-known adaptations for this unique task include the characteristic secondary wall thickenings, forming rings and helices. A new, clearly distinct structural element containing glycine-rich proteins is now visualized for the first time, using confocal laser scanning microscopy in the mature protoxylem of elongating organs of seed plants. This structural element is arranged along the longitudinal axis of the protoxylem elements. It interconnects the secondary wall thickenings within and between protoxylem elements, as well as the protoxylem with other cell types such as xylem parenchyma cells and metaxylem elements. The structural element is stable against detergent extractions, proteinase, pectinase and cellulase hydrolysis, and is closely associated with rhamnogalacturonan-I, a pectic polysaccharide. The results clearly demonstrate that the cell wall of protoxylem cells is a highly dynamic and complex structure. The typical polysaccharide-rich primary wall of living and elongating plant cells is progressively modified and finally replaced by a protein-rich wall in the dead and passively stretched protoxylem elements. These glycine-rich walls originated early in the evolution of the seed plants as confirmed by the analysis of genomic information.

Supplemental data available online

Key words: Extracellular matrix, Glycine-rich cell-wall protein, Plant anatomy, Protoxylem, Rhamnogalacturonan I, Seed plants (spermatophytes)

Introduction

Proteins of the extracellular matrix in animal cells or the cell wall in plant cells have only evolved after the divergence of plants and animals, about 1 billion years ago during the Precambrian. Although the cell walls of seed plants are mainly composed of polysaccharides such as cellulose, hemicelluloses and pectins, they also contain variable amounts of structural proteins. These proteins have traditionally been classified as glycine-rich proteins (GRPs), proline-rich proteins (PRPs) and hydroxyproline-rich proteins (HRGPs). With the exception of GRPs, they are glycosylated and contain hydroxyproline (Carpita and Gibeaut, 1993; Cassab, 1998; Zablackis et al., 1995). Dividing and elongating plant cells contain very little cross-linked structural cell-wall proteins. As a rule, cell-type- and tissue-specific cross-linking of these proteins into the cell wall occurs towards the end of elongation growth. Little is known about the roles of these proteins. It is thought that they strengthen the cell walls in normal plant development (Fry, 1988; Carpita and Gibeaut, 1993) and are involved in incompatible plant-pathogen interactions (Lamb and Dixon, 1997; Delledonne et al., 1998).

Xylem is the principal water-conducting tissue of vascular plants. It contains water pipes formed by the walls of dead cells. To allow the efficient transport of water and solutes, the end walls of the cylindrical cells are perforated (in vessel members) or the ends are elongated and make contacts side by side (in tracheids) by numerous pit pairs. Vessel members are absent from most gymnosperms but are typically observed in the wood of angiosperms. However, the xylem of elongating organs of angiosperms often contains both cell types. For convenience, they are collectively called 'tracheary elements' (Esau, 1977). The main steps of the differentiation of tracheary elements are cell elongation, strengthening of the wall by deposition of secondary wall layers, lignification and programmed cell death initiated by the collapse of the vacuole and followed by the degradation of cellular constituents by vacuolar hydrolases (Groover et al., 1997; Groover and Jones, 1999; Fukuda, 2000). Finally, the hydrolysis products are probably taken up by the living xylem parenchyma surrounding the tracheary elements.

Protoxylem is the water-conducting tissue of young and elongating plant organs, whereas metaxylem starts to differentiate only towards the end of elongation growth. The challenge for the growing plant is to maintain a functional water-conducting system made up of the cell walls of dead protoxylem elements (PX) embedded in rapidly elongating xylem parenchyma cells. The adaptations evolved by the seed plants to comply with this task are not yet completely

understood. The characteristic ring- and helix-shaped secondary wall thickenings (SW) contain lignin and allow a considerable, passive elongation of the dead PX. The passive elongation is further facilitated by the fact that the PX only lignify their SW, whereas the primary walls remain unlignified. There is evidence that the unlignified primary walls are partially hydrolysed before the execution of the cell death program, facilitating the passive elongation of the PX (Esau and Charvat, 1978; Ryser, 2003). The remaining primary wall residues with a characteristic fibrous ultrastructure were thought to have no further functions and to be diluted by their passive elongation (O'Brien, 1981).

Recently, it has been shown that the primary walls of dead PX contain glycine-rich, structural cell-wall proteins (Keller et al., 1989; Ryser and Keller, 1992; Ryser et al., 1997). Based on sectioned material, a model was developed that illustrates the arrangement of the GRPs in the protoxylem of bean and soybean hypocotyls (Ringli et al., 2001a). There, the GRP-containing cell-wall material (GRPCWM) forms the wall between two PX and interconnects the ring- and helix-shaped SW. In addition, the SW of the PX are also connected with the middle lamella of the surrounding xylem parenchyma cells. Thus, GRPCWM is suggested to form a three-dimensional (3D) network, stabilizing the whole protoxylem. The model proposes a structural function for the GRPCWM: by fixing the ring- and helix-shaped SW in their correct position, it inhibits the tilting of the ring-shaped SW and the compression of the helical ones, thus inhibiting the premature collapse of the protoxylem. The deposition of the GRPCWM starts in the cell corners of the PX in close association with pectin (Ryser, 2003). Pectin is a major component of primary cell walls of land plants and encompasses a range of galacturonic-acid-rich polysaccharides. Three major pectic polysaccharides are homogalacturonan, rhamnogalacturonan I (RG-I) and rhamnogalacturonan II. They are thought to occur in all primary cell walls and are possibly covalently linked (Willats et al., 2001).

In the present paper, the 3D structure of GRPCWM is visualized with confocal laser scanning microscopy (CLSM). The structural function of GRPCWM is experimentally tested by isolating PX, followed by enzymatic hydrolysis and detergent extractions. Finally, it is shown that the GRPCWM originated early in the evolution of seed plants.

Materials and Methods
Plants, growth conditions, and organs used for the experiments
Dicotyledonous plants

For *Glycine max* L. (cv. Paradies; Wyss Samen, Switzerland), seeds were soaked in water for 5 hours and grown at room temperature in the dark. Hypocotyls with a length of 5-7 cm were used for the experiments and ~1 cm long pieces were dissected from the apical, middle and basal regions of the hypocotyl for the experiments.

For *Arabidopsis thaliana* L., accession Columbia, germinating seeds were grown under sterile conditions on half-strength Murashige and Skoog medium (Sigma) containing 0.7% Bacto agar, at 20-22°C and 60% humidity in the dark. For the experiments 1-2-cm-long hypocotyls were used.

For *Nicotiana tabacum* L., cv. Xanthi, germinating seeds were grown under the same conditions as *Arabidopsis*, and 0.6-1.3 cm long hypocotyls were used for the experiments.

Monocotyledonous plants

Leucojum vernum L. and *Galanthus nivalis* L. were grown in the Botanical Garden of the University of Fribourg. Segments of the floral axis below the bract with a length of ~1 cm (*Leucojum*) and between the bract and the flower with a length of ~3 cm (*Galanthus*) were used for the experiments.

Gymnosperms

Pinus sylvestris L. and *Picea abies* L. seeds were harvested from a nearby forest, planted in forest soil and grown in a greenhouse maintained at a minimal night temperature of 13-15°C. Cotyledons with a length of 2 cm and the upper half of 2-cm-long hypocotyls were used for the experiments.

Isolation of PX for 3D reconstruction by CLSM

For the visualization of the 3D structure of the GRPCWM in PX, hypocotyl segments were peeled, cut into smaller pieces and softened with crude pectinase from *Rhizopus* sp. (Poly-1,4-α-D-galacturonide-glycanohydrolase; Sigma-Aldrich) or pectinase followed by driselase from *Basidiomycetes* sp. (Fluka) containing carboxymethylcellulase, pectinase, xylanase, dextranase, laminarinase, amylase, protease and further lytic and macerating activities. Similar results were obtained with the two methods. Pectinase was used at 5 U ml^{-1} in sodium-acetate buffer pH 5.2 containing sorbitol (0.2 M) and NaN$_3$ (0.02%). Driselase (2%) was dissolved in the same buffer as pectinase and then filtered through Whatman glass fibre filters (GFA). In all experiments, 1 ml of enzyme solution was used for a 1 cm segment of a soybean hypocotyl or an equivalent amount of other plant materials. The enzymatic hydrolysis of the samples was performed at 37°C with continuous shaking at 200 rpm for 17 hours. The samples were then either processed directly for immunostaining or fixed in 30% ethanol.

Antibodies

GRP1.8 is a polyclonal rabbit antibody raised against a fusion protein containing amino acids 15-333 of the GRP1.8 of *Phaseolus vulgaris* (Keller et al., 1988). JIM5 is a rat monoclonal antibody raised against homogalacturonans that recognizes homogalacturonans with a low degree of methylesterification (Knox, 1997; Willats et al., 2000). JIM7 is a rat monoclonal antibody raised against homogalacturonans that recognizes homogalacturonans with a higher degree of methylesterification (Knox, 1997; Willats et al., 2000). CCRC-M1 is a mouse monoclonal antibody (IgG$_1$) recognizing a terminal fucosyl residue present primarily on xyloglucan and, to a lesser extent, on RG-I (Freshour et al., 1996). CCRC-M2 is a mouse monoclonal antibody (IgM) recognizing RG-I whose epitope has not yet been characterized in detail (Freshour et al., 1996). Polyclonal antibodies were used that target a mixed guaiacyl-syringyl (GS) lignin dehydrogenation polymer (Ruel et al., 1994; Joseleau and Ruel, 1997).

Immunostaining

Small tissue pieces or isolated PX were first incubated with NH$_4$Cl for 15 minutes and then with primary antibodies for 2 hours in TBST (20 mM Tris, 50-500 mM NaCl, 0.1% Tween 20, pH 7.5) at room temperature, washed three times with TBST and finally incubated for 1 hour with the appropriate secondary antibodies. The NaCl concentration was 500 mM for GRP1.8, 50 mM for JIM5 and JIM7, and 150 mM for CCRC-M1 and CCRC-M2. Primary antibodies were diluted 1:1000 (GRP1.8), 1:10 (JIM5 and JIM7) or 1:2 (CCRC-M1 and CCRC-M2). GRP1.8 was detected with goat anti-rabbit Alexa Fluor 488, JIM5 and JIM7 with goat anti-rat Alexa Fluor 488, and CCRC-M1 and CCRC-M2 with goat anti-mouse Alexa Fluor 488, all at a dilution of 1:1000 in TBST, using the same salt concentration as for the primary antibodies. In the controls, rabbit serum (1:1000)

replaced GRP1.8 antibodies. The staining with JIM5 was specifically inhibited with 500 mM NaCl (Ryser, 2003). Additional controls for monoclonal antibodies were JIM7 and CCRC-M1, because they did not stain isolated PX.

Staining of lignin, cellulose and cell-wall protein

Lignified cell walls were stained with ethidium bromide (0.0025% in Tris-HCl 20 mM, pH 7.5) for 10 minutes and washed two or three times in buffer. The nucleic acid stain ethidium bromide also selectively stains cell walls containing lignin or other phenolic compounds (O'Brien and McCully, 1981). β-Glucans were stained with 0.1% Calcofluor White ST (Cyanamid) in distilled water for 15 minutes and washed for 5 minutes in distilled water (Maeda and Ishida, 1967; Wood et al., 1983). Cell-wall proteins were stained with Coomassie Blue R-250. The staining solution was prepared with 0.25% Coomassie Blue in methanol (40%) and acetic acid (10%), and filtered. Staining was performed for 6 minutes, followed by rinses in methanol (40%) acetic acid (10%) four times for 2 minutes each and in distilled water.

Microscopy

Preparations were first studied with a Leica DMR HC microscope, equipped with a digital camera (Axiocam; Carl Zeiss, Microscopy, Jena, Germany). For epifluorescence and confocal microscopy, standard filter combinations for fluorescein and rhodamine were used for Alexa Fluor 488 and ethidium bromide, respectively. Confocal images were taken with a BioRad MRC 1024 microscope equipped with a Kr/Ar laser. z-Series of pictures were taken at intervals of 1 μm, resulting in stacks of 15-44 images. Image analysis was performed on a Macintosh computer by using the public domain NIH Image program (developed at the US National Institutes of Health and available on the Internet at http://rsb.info.nih.gov/nih-image/). Adobe PhotoShop was used for image pseudocolouring.

Isolation and purification of PX

To enrich GRPCWM for microscopy and amino acid determinations, peeled hypocotyls were rinsed with tap water, boiled for 5 minutes in distilled water containing ascorbate (10 mM). The hypocotyl segments to be analysed were then removed and cut into smaller pieces with razor blades. Finally, the tissue pieces were homogenized with a Polytron homogenizer (PT-MR2100, Kinematica, Switzerland) at 20,000 rpm for 1 minute in 20 ml of pectinase buffer containing ascorbate (10 mM). After pectinase digestion, the homogenate was collected by centrifugation (3300 **g** at 4°C for 25 minutes), washed and digested by driselase (containing 10 mM ascorbate). After transfer to Tris-HCl buffer (0.02 M, pH 7.5, containing 0.02% NaN$_3$), the crude cell walls were homogenized once more at 20,000 rpm for 30-60 seconds. GRPCWM was then enriched by magnetic separation using Captivate Ferrofluid conjugates (Molecular Probes) with GRP1.8 (1:1000) as primary antibody followed by either goat anti-rabbit Captivate Ferrofluid conjugates (3 μg per hypocotyl segment) or goat anti rabbit DSBX-Biotin (1:1000), and finally by streptavidin Captivate Ferrofluid conjugates (3 μg per hypocotyl segment). The magnetic separations were performed in Eppendorff or 10 ml tubes using a Magnetight Separation Stand (Novagen). DSBX-biotin and streptavidin were separated twice with biotin for 60 minutes each. Biotin (50 mM) was dissolved in NaCO$_3$ (10 mM) and diluted 1:4 with TBST containing 150 mM NaCl. Finally, the PX fraction was extracted with boiling SDS (2%) in TBST containing NaCl (150 mM) and 1,4-dithio-DL-threitol (75 mM). Unexpectedly, the isolated PX and the Captivate Ferrofluid particles could not be separated by this procedure. Even after six separations, the bulk of PX remained associated with the Captivate Ferrofluid particles. Increasing the salt concentration to 500 mM NaCl did not give better results.

Enzymatic degradation of isolated PX

Isolated PX were digested with 0.1% proteinase K (Merck) in Tris-HCl 20 mM, pH 7.5, containing NaN$_3$ (0.02%) and with 500 U ml^{-1} cellulase (endo-β-1,4-glucanase of *Trichoderma* spec., Megazyme) in sodium acetate, 50 mM, pH 4.8, containing NaN$_3$ (0.02%). The cellulase is used to produce oligosaccharides from xyloglucan and slowly attacks crystalline cellulose (Avicel).

Amino acid analysis of cell-wall fractions

The amino acid composition of different cell-wall preparations was determined with an Aminoquant amino acid analyser (Agilent Technologies, Palo Alto, California) after hydrolysis of the samples with 6 M HCl for 22 hours at 110°C under argon. The analyses were performed by the Protein Analysis Unit of the Institute of Biochemistry of the University of Zürich (P. Hunziker). Unless otherwise stated the results correspond to the mean of two independent determinations.

Screening for plant sequences structurally similar to the *GRP1.8* gene

GRP1.8-related genes were identified from a plant nucleotide sequence database downloaded from the TAIR web site (of May 2003: 3,963,577 sequences with 3 billion total letters, ftp://tairpub:tairpub@ftp.arabidopsis.org/home/tair/Sequences/blast_datasets/). Databases and BLAST algorithms (Altschul et al., 1997) were locally installed. The nucleotide sequence encoding glycine-rich cell-wall protein *GRP1.8* from *P. vulgaris* (accession number X13596) was used as the query sequence to screen the sequence database with the TBLASTN algorithm. Results were parsed and subsets of positive sequences were selected according to the following parameters: (i) presence of a similarity with *GRP1.8* from bean for both the signal peptide and the glycine-rich region; (ii) presence of GX repeats for which G residues represent more than 40% of the putative protein; (iii) presence of several Y residues (>3.2% of the putative protein); (iv) presence of a low content of F residues (<2.5%).

Sequence analysis of putative *GRP1.8* genes in plants and phylogenetic analysis

The retrieved sequences were analysed using the GCG Sequence Analysis Software (version 10.3) and the EMBOSS package (http://www.hgmp.mrc.ac.uk/Software/EMBOSS/). A subset of positive sequences was translated in the three frames to check for the presence of stop codons and to calculate the length of the putative protein. Selected candidates were used as query for a second round of TBLASTN search. Prediction of the subcellular localization of putative genes was performed using the internet version of PSORT prediction (http://psort.nibb.ac.jp/form.html).

Sequence alignments were performed with PILEUP (gap creation penalty=0, gap extension penalty=1). Phylogenetic analysis was performed with ClustalW (Thompson et al., 1994), using the neighbour-joining method. Confidence value for the nodes was calculated using 1,000 bootstraps.

Results
3D visualization of the GRP network with CLSM

Enzymatically softened tissue pieces from different regions of the hypocotyl were incubated with bean GRP1.8 polyclonal antibodies and stained with Alexa Fluor 488 secondary antibody conjugates (green fluorescence). The lignified cell walls were stained with ethidium bromide (red fluorescence). In the apical region of the hypocotyl, the ring- and helix-shaped

Fig. 1. 3D reconstruction of PX in different regions of soybean hypocotyls. (A-E) Apical region of the hypocotyl. (A) PX with ring-shaped, lignified SW (red fluorescence) and GRPCWM (green fluorescence) interconnecting the lignified SW. (B) PX with a helical, lignified SW. The attachments of the GRPCWM are clearly visible and are often somewhat broadened along the lignified SW thickening (arrow). (C) Two PX. The younger one, with closely spaced SW, does not yet contain GRPCWM. The older one is characterized by more widely spaced SW and the typical strands of the GRPCWM. The wall between the two is also clearly fluorescent (arrows). (D) The ends of two PX joined together end-by-end. The arrows indicate the GRP-containing wall connecting these two cells with a third PX (not retained in the preparation). The same type of wall, seen here in front view, is seen in (C) in side view. The ends of the two PX are outlined with a hatched line. (E) Rabbit serum control: no green fluorescence is observed. Ethidium bromide stains the SW and (very faintly) the GRPCWM. Notice the small protuberances on the SW in the direction of the longitudinal axis of the hypocotyl (arrows). (F) Middle region of the hypocotyl: PX with strongly elongated helical SW. Notice the stress-fibre-like appearance of the GRPCWM and the attachments between the GRPCWM and the SW (arrows). In contrast to the apical region of the hypocotyl, where the GRPCWM spans only the distance between adjacent SW, long, continuous filaments or sheets are typically observed in the mature regions of the hypocotyl (arrowheads). (G-I) Basal region of the hypocotyl. New MX are differentiating but the structure of the PX remains much the same as in the middle region of the hypocotyl. (G) Three stretched helical SW are visible to the left and a newly formed PX with a flat helical SW to the right. Notice the GRPCWM along the helical SW of this PX. Arrows indicate a faintly stained cell corner. (H) Overview, showing (from left to right) a MX (m) and a series of younger to older PX. The older elements are characterized by passively elongated helical SW and intense staining with GRP1.8 antibodies. Little staining is observed in the MX, with the exception of a cell corner adjacent to the youngest PX (arrow). (I) Rabbit serum control: no green fluorescence is observed. Ethidium bromide stains the SW and, faintly, the GRPCWM (arrows). Bars, 10 μm.
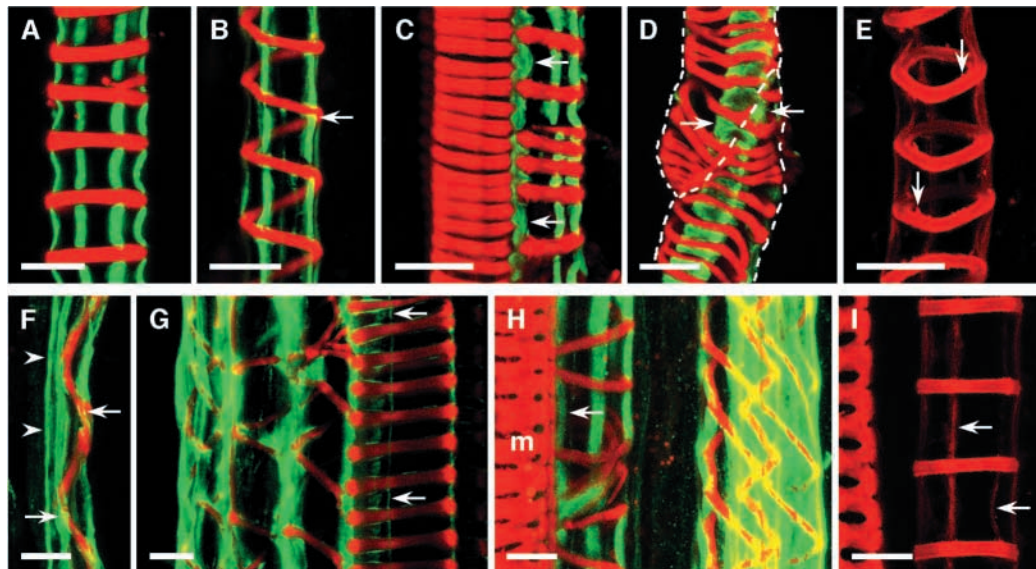
SW are interconnected with several filaments of GRPCWM (Fig. 1A,B). The filaments are arranged in straight lines along the longitudinal axis of PX. However, they do not cross the SW. A slightly broadened zone of contact is often observed between the SW and the GRPCWM. Younger PX are characterized by closely associated SW and by the absence of GRPCWM filaments (Fig. 1C), confirming that lignification precedes the deposition of GRPCWM (Ryser et al., 1997; Ryser, 2003). The wall between the younger and the older PX is stained with GRP1.8 antibodies, and forms a sheet-like structure between the two cells (Fig. 1C,D, arrows). At the regions where two PX are connected end-by-end (Fig. 1D), the SW are often more narrowly spaced and interconnected than in the rest of the PX. GRPCWM occurs regularly in this region. However, no additional GRP-containing structures are observed specifically interconnecting the two ends of the PX.

In the middle region of the hypocotyl, several new PX and the first metaxylem elements (MX) have differentiated (Ryser, 2003), indicating that the middle and more basal regions of the hypocotyl are no longer elongating. The oldest PX are passively elongated in these regions, as shown by the displacement of the ring-shaped SW and the stretched appearance of the helical ones (Fig. 1F). Staining with GRP1.8 antibodies is intense in the oldest PX (Fig. 1F-H). The MX remain unstained, with the exception of the cell corners between MX and PX (Fig. 1H). The GRPCWM in these more mature regions of the hypocotyl forms long filaments, following the cell corners, whereas, in the apical region, the GRPCWM just interconnects the SW. GRPCWM is, therefore, deposited at different developmental stages along a single PX, indicating a tight regulation of this process, depending on the presence of SW.

A model summarizing the development and 3D arrangement of GRPCWM in the protoxylem of soybean hypocotyls is presented in Fig. 2.

Isolation of PX

To test the mechanical properties of the newly described 3D structures of the GRPCWM, fragments of PX were isolated. Small tissue pieces, digested with pectinase and driselase, were homogenized and a crude cell-wall preparation was recovered by low-speed centrifugation. The crude cell walls were then further purified by a magnetic separation procedure using GRP1.8 antibodies followed by Captivate Ferrofluid conjugates and magnetic separators. The purity of the fractions obtained is documented in Fig. S1 (http:// jcs.biologists.org/supplemental/). Typical, medium-sized fragments of PX obtained with this method are shown in Fig. 3A. A part of the GRPCWM was separated from the SW. However, a closer inspection of the fragments revealed that, as a rule, small amounts of GRPCWM remained associated with the SW (Fig. 3A,B). This observation indicates that the connection between GRPCWM and SW is mechanically strong, although GRPCWM is preferentially

Fig. 2. Schematic representation of the 3D arrangement of GRPCWM in the protoxylem of soybean hypocotyls. (A) Differentiating PX at the top of the hypocotyl. (B) Mature protoxylem in the middle of the hypocotyl. Green shows GRP-containing structures. Red shows lignified secondary wall thickenings. Differentiation of the cells occurred from left to right. Therefore, the oldest protoxylem element is located at the left and the metaxylem element (m) at the right. A comparison between the two oldest PX in (A,B) shows their passive elongation and the continued deposition of GRPCWM in the dead cells. The nonextensible metaxylem elements do not contain GRP, except in the cell corners shared with protoxylem elements.
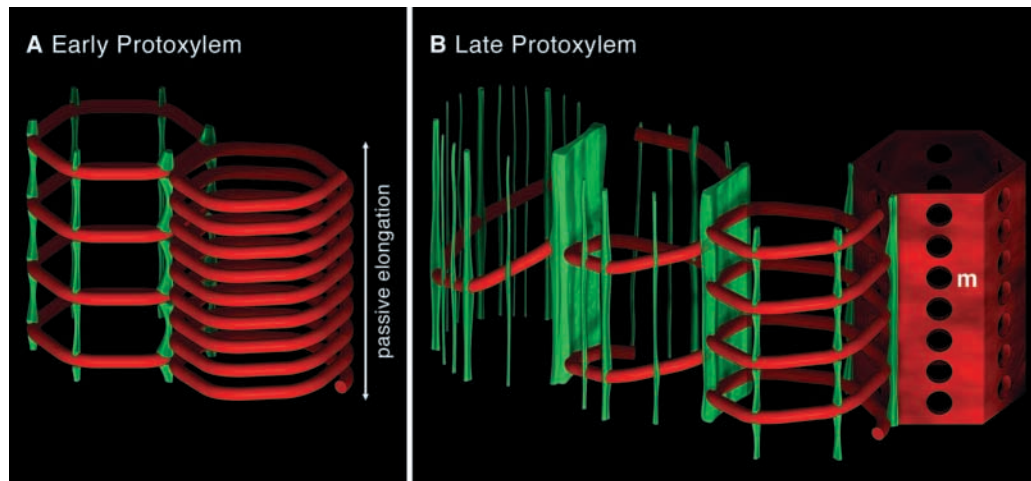

A Early Protoxylem

B Late Protoxylem

passive elongation

m

Table 1. Stability of PX with ring-shaped SW from the apical region of the hypocotyl

	Interconnected ring-shaped SW (%)*	
	Buffer control	Enzyme
Proteinase K treatment	53	52
	62	50
Cellulase treatment	56	75
	66	50

*At least 200 rings were counted per experiment.
The results of two independent determinations are shown.

fractured near its attachment to the SW. Sometimes, the GRPCWM of isolated PX was compressed by helical SW (Fig. 3C), indicating that the GRPCWM is flexible. The helical SW might act as a coil spring, counteracting the forces promoting elongation of the hypocotyl.

## Effect of SDS and enzymatic hydrolysis on isolated PX

Isolated PX were extracted with SDS or treated with proteinases and cellulase to analyse whether the stability of GRPCWM depends on protein or polysaccharides. The enzyme treatments were followed by a SDS extraction to inactivate enzyme activities (Fig. 4A-F). After digestion with proteinase K, the intensity of the fluorescence was reduced without apparently affecting the stability of the GRPCWM. Similar negative results were obtained with collagenase that specifically degrades GRP1.8 fusion protein fragments (Ryser et al., 1997; Ringli et al., 2001b). A quantitative and sensitive estimate of the stability of GRPCWM was obtained by counting free and GRPCWM interconnected ring-shaped SW at the apical region of the hypocotyl. Free ring-shaped SW are produced by the action of pectinase and driselase on younger PX with SW not yet interconnected by GRPCWM. In older PX, SW can be separated from the GRPCWM by the shearing forces of the homogenisation procedure. The effect of proteinase K and cellulase on the number of free ring-

shaped SW is shown in Table 1. The number of free rings is not increased by the enzyme treatments, confirming the stability of GRPCWM towards these treatments. These results are not quite unexpected, because the driselase used for the isolation of PX already contained cellulase and proteinase activities. Nevertheless, they indicate that the enzymatic digestion was allowed to come to completion. Therefore, it can be concluded that proteinase K, collagenase, cellulase and pectinase digestions, as well as SDS extractions are not able to destroy GRPCWM and its connections with SW.

Amino acid composition of isolated PX

The amino acid composition of crude cell walls and purified PX was determined for the apical and middle region of hypocotyls (Table 2). The molar concentration of glycine was increased two to three times in the PX fraction compared with crude cell walls and reached 23-32 mole %. This observation confirms that the GRP1.8 antibody interacts specifically with a GRP in PX, and that this protein is highly enriched in the GRPCWM associated with PX. Only trace amounts of hydroxyproline were found in the apical region of the hypocotyl but, in the middle region of the hypocotyl, the amount of this amino acid was increased by a factor of 16. Interestingly, hydroxyproline was quantitatively recovered in the PX fraction, indicating that cell-wall-bound hydroxyproline is specifically associated with lignifying and lignified cell walls of the protoxylem at this stage of development. In addition, considerable amounts of mono- and oligomeric hydroxyproline were present in the crude cell-wall fraction (U. Ryser et al., unpublished). Proline, the precursor of hydroxyproline, accumulates only by a factor of two from the apical to the middle region of the hypocotyl, and is not significantly increased in the PX fraction compared with crude cell walls. The amino acid composition was also determined for the DSBX-biotin streptavidin Captivate Ferrofluid conjugates used for the purification of PX. No significant contamination of the PX fraction results from the proteins associated with these conjugates.

Fig. 3. Soybean PX fragment after prolonged homogenization. Some typical medium-sized fragments from the apical region of the hypocotyl are shown in (A-C). (A) Two lignified rings are interconnected with GRPCWM. A separation
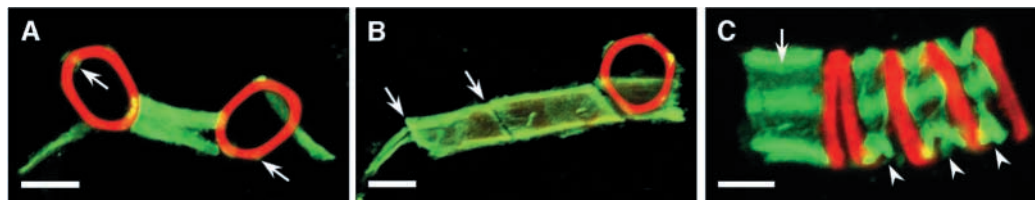
between the SW and the GRPCWM occurs preferentially near the lignified SW. However, some GRPCWM remains associated with the lignified SW (arrows), indicating that the SW and the GRPCWM are linked very tightly together. (B) The GRPCWM between two PX is still associated with a ring-shaped SW. Two other rings are missing but their original position remains visible (arrows). (C) Compression of the GRPCWM was sometimes observed between helical SW (arrowheads), whereas, at the end of the fragment, the GRPCWM is present in an extended form (arrow). The compression of the GRPCWM is explained by a shortening of the helical SW. Bars, 10 μm (A,B); 5 μm (C).

Table 2. Amino acid composition of isolated cell wall and protoxylem fractions

| | Apical region of hypocotyl | | | | Middle region of hypocotyl | | | | DSBX-biotin ferrofluid | |
| | Cell walls | | Protoxylem | | Cell walls | | Protoxylem | | | |
Amino acid	nmol*	%[†]	%[‡]	%[†,§]	nmol*	%[†]	nmol*	%[†]	nmol*	%
Asp	40.3	10.0	10.9	9.2	85.1	9.7	1.4	1.1	17.2	10.9
Glu	41.3	10.3	11.3	9.1	82.6	9.4	1.8	1.5	19.8	12.6
Ser	28.6	7.1	13.8	8.6	64.1	7.3	15.8	12.5	13.5	8.6
His	0.0	0.0	0.0	0.0	0.0	0.0	0.0	0.0	3.3	2.1
Gly	42.4	10.6	23.0	32.3	110.4	12.6	36.1	28.6	12.7	8.1
Thr	19.8	4.9	4.7	3.9	41.9	4.8	3.7	3.0	15.2	9.7
Ala	36.2	9.0	7.1	10.4	80.6	9.2	9.0	7.1	16.0	10.2
Arg	16.6	4.1	2.6	3.2	29.6	3.4	1.9	1.5	6.6	4.2
Tyr	14.0	3.5	1.5	2.4	27.7	3.2	3.0	2.3	4.5	2.9
Val	29.5	7.4	4.8	4.0	61.2	7.0	5.4	4.3	10.8	6.9
Met	9.2	2.3	0.4	1.6	17.5	2.0	0.9	0.7	0.1	0.1
Phe	22.1	5.5	2.5	1.7	45.6	5.2	3.2	2.5	4.2	2.7
Ile	25.3	6.3	3.1	2.4	51.7	5.9	3.6	2.9	3.6	2.3
Leu	42.3	10.5	5.2	0.0	85.9	9.8	5.3	4.2	11.9	7.6
Lys	15.4	3.8	4.4	4.9	34.6	3.9	5.3	4.2	11.1	7.1
Pro	18.1	4.5	4.7	6.2	42.8	4.9	6.1	4.8	6.6	4.2
4-HO-Pro	0.5	0.1	nd	0.0	14.3	1.6	23.7	18.7	0.0	0.0
Trp	0.0	0.0	0.0	0.0	0.0	0.0	0.0	0.0	0.0	0.0
Total	401.6	100.0	100.0	100.0	875.6	100.0	126.2	100.0	157.1	100.0

*nmol per hypocotyl per cm.
[†]Isolated with GRP1.8 as primary antibody, followed by a DSBX-biotin secondary antibody conjugate and Captivate Ferrofluid streptavidin conjugate.
[‡]Isolated with anti-GRP1.8 as primary antibody and Captivate Ferrofluid secondary antibody conjugate.
[§]Single determination; all other values correspond to the mean of two independent determinations.
nd, not determined.

Cytochemistry of GRPCWM

The GRPCWM is specifically stained by Coomassie Blue (Fig. 5A). The lignified cell walls of the xylem remain unstained, as do the cell walls of elongating plant cells, which are composed mainly of polysaccharides (result not shown). Calcofluor White selectively stains β-glucans and crystalline cellulose (Maeda and Ishida, 1967; Wood et al., 1983). In isolated PX, mainly the SW and cell-wall fragments of various other cell types were stained with Calcofluor White. The fluorescence is intense in unlignified or only partially lignified SW, and much weaker in lignified SW. A weak and rather diffuse staining is also observed in the GRPCWM (Fig. 5B). After proteinase K or collagenase digestion, the staining of GRPCWM with Calcofluor White was no longer detectable. It is not clear whether this effect is due to the action of the proteases themselves or to the SDS treatment following the enzyme treatment. However, the results clearly indicate that cellulose is not a major constituent of the GRPCWM. Pectins were detected in the GRPCWM by immunogold labelling with JIM5 and JIM7 monoclonal antibodies (Ryser, 2003). Applied to isolated PX, JIM5 recognized mainly structures at the apex of PX that were not stained with GRP1.8 antibodies (Fig. 5C, arrow). GRPCWM was only labelled in the apex of PX or in the youngest PX. In older PX, GRPCWM was not labelled at all with JIM5 (Fig. 5E). The staining with JIM7 was completely negative if applied to isolated PX. The monoclonal antibody CCRC-M2 recognizes an unknown epitope on RG-I and consistently stained the GRPCWM in the apical and middle region of the hypocotyl (Fig. 5I). Interestingly, the staining patterns of CCRC-M2 were identical to those observed with GRP1.8 antibodies. No staining of the PX was observed with the monoclonal antibody CCRC-M1, confirming that xyloglucan is not a quantitatively important constituent of GRPCWM (Ryser, 2003). Antibodies raised against a mixed guaiacyl-syringyl (GS) lignin dehydrogenation polymer did not stain the GRPCWM, confirming earlier results (Ryser et al., 1997). These observations indicate that GRPCWM does not contain lignin (data not shown).
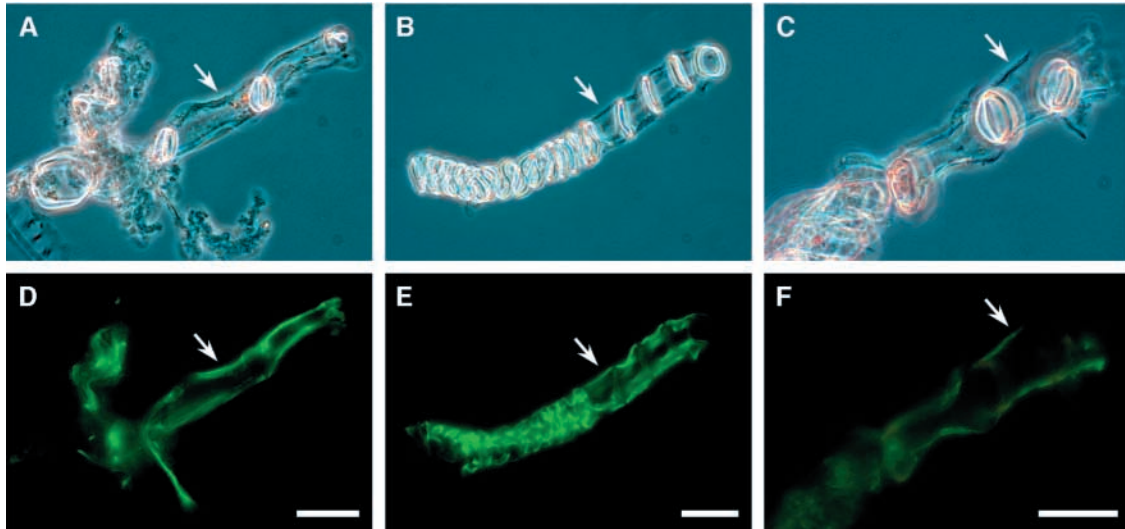
Fig. 4. Enzymatic digestion of isolated soybean PX. Isolated PX with widely spaced ring-shaped SW are compared after different treatments. (A,D) Buffer control. (B,E) Cellulase. (C,F) Proteinase K. (A-C) Phase contrast microscopy; arrows indicate GRPCWM. (D-F) Epifluorescence microscopy of the same PX as shown in (A-C). The arrows indicating GRPCWM are located at the same positions as in (A-C). The ring-shaped SW remain connected after all three treatments. However, the intensity of the fluorescence is reduced after the treatment with proteinase K. Bars, 20 μm.

Occurrence of GRPCWM in seed plants

Among dicotyledonous plants, etiolated hypocotyls of *A. thaliana* and *N. tabacum* were studied with epifluorescence and CLSM using bean anti-GRP1.8 as primary antibody to detect GRPCWM (Fig. 6A,B). Images very similar to those from soybean hypocotyls were obtained. Among monocotyledonous plants, the mesocotyl and the coleoptile of etiolated *Avena sativa* seedlings were examined with the same methods. Although many ring-shaped SW were observed in the preparations, GRPCWM could not be visualized either with GRP1.8 antibodies or after Coomassie-Blue staining (data not shown). A sudden and rapid elongation of the floral axis is observed in many plant species after the initiation of the reproductive state. Among monocots, well-known examples are the flowering structures of grasses and of bulbous plants. For our experiments, *Leucojum vernum* and *Galanthus nivalis* were selected. In both species, GRPCWM was visualized with bean GRP1.8 antibodies. Again, structures very similar to those of soybean were observed (Fig. 6C-E). The hypocotyls of gymnosperms elongate slowly (weeks instead of days as in dicots). Furthermore, their elongation is not promoted by etiolation. Only a few PX are formed before cambium-dependent differentiation of secondary xylem is initiated. Extremely thin and weakly fluorescent filaments were detected with bean GRP1.8 antibodies in the PX of the gymnosperms examined (Fig. 6G-I). Filaments in PX and cell corners in other cell types of the xylem stained with Coomassie Blue (Fig. 6J). It is concluded that GRPCWM is a newly described structural element commonly occurring in seed plants.

Screening of plant sequences for genes similar to *GRP1.8*

To identify genes similar to *GRP1.8* from *P. vulgaris* in plant nucleotide sequences, a 'sub-protein' search strategy was used. In order to focus the analysis on structural proteins localized to the cell wall, the first 89 amino-acid N-terminal residues from the 465 residues of GRP1.8 were used to perform the searches. The fragment contains a predicted N-terminal peptide for an extracellular localization, a glycine-rich fragment of 57 amino acids (63% of glycine residues) and six tyrosine residues. For further investigation, a subset of sequences showing homology all along the query sequence was analysed for the presence of open reading frames and was translated into amino-acid sequences. From the chosen sequences, proteins similar to the protein structure of GRP1.8 were selected using the following criteria: (i) presence of a signal peptide for a predicted extracellular or vacuolar localization; (ii) amino-acid composition of more than 40% of glycine residues; (iii) presence of several tyrosine residues which are spread all over the protein (>3.2%); and (iv) presence of a low amount of phenylalanine residues (<2.5%). From the BLAST analysis, a subset of 80 sequences was selected. From these 80 selected sequences, 20 were retained following the criteria of structural similarity with the GRP1.8 protein. The rest of the sequences were rejected either because of structural criteria or because a very similar sequence from the same species was already selected (data not shown). The 20 sequences showing homology with the bean GRP1.8-encoding gene were from ten different species, including monocots and dicots. Six of them have already been characterized and come from barley (*hvGRP*), maize (*ZmGRP3*), rice (*CAI1* and *GRP 0.9*), rape (*BNGRP22*) and bean (*GRP1*) species. 14 GRP genes have not yet been characterized as structural genes with a similarity to the bean *GRP1.8* gene; these come from *Arabidopsis*, kale, barley, wheat, sorghum, rice and maize (Table 3). Information from expressed sequence tag databases indicates that GRPs also commonly occur in gymnosperms.

Fig. 5. Cytochemistry of the GRPCWM of soybean PX. (A-D,H,I) Apical region of hypocotyls. (E-G) Middle region of hypocotyls. (A) Differential interference contrast microscopy, Coomassie-Blue staining. The GRP-containing filaments of the PX are strongly stained (arrow). With this technique, an optical section is obtained. Therefore, not all GRP-containing filaments are visible in a single plane of focus. A similar PX is shown in Fig. 1A after staining with a GRP1.8 probe. (B) Calcofluor stains cell-wall fragments of different cell types (arrowheads) and the lignified SW of PX. Filaments corresponding to GRPCWM (arrow) are only weakly stained with Calcofluor. (C) JIM5 monoclonal antibodies consistently stain the ends of PX (arrow), thus staining components not being stained with GRP1.8 antibodies, as well as the cell corners (arrowheads) commonly stained with GRP1.8 antibodies. (D) Control preparation, treated with 500 mM NaCl inhibiting specifically the staining with JIM5. (E) JIM5 monoclonal antibody. Two mature PX are shown, together with a differentiating reticulated tracheary element. The SW of the latter are only weakly stained with ethidium bromide, indicating that lignification of the SW is not yet complete. The cross-wall between the reticulated tracheary element and the younger PX is stained with JIM5 antibodies but not the cross-wall between the younger and the older PX. The GRPCWM is only occasionally stained (arrow) in the younger PX, whereas the older PX with the elongated helical SW remains almost unstained. Arrowheads indicate a faint staining of the cell corners of the reticulated xylem element. (F) The ends of two immature MX are clearly stained with JIM 5 monoclonal antibodies (arrows), as are some cell corners (arrowheads). (G) Enlarged view of the zone of contact between two MX. A thin region between the two MX is stained with JIM5. (H) No staining of the isolated PX was observed with the CCRC-M1 monoclonal antibody, which specifically stains xyloglucan. Therefore, this antibody can serve as a control for the CCRC-M2 monoclonal antibody staining RG-I. (I) PX with helical SW stained with CCRC-M2. The GRPCWM between two PX (arrowheads) and in the cell corners is stained. CCRC-M2 stains the same structures as the GRP1.8 probe in the protoxylem. In addition, cell-wall fragments of other cell types present in the preparation are also stained (arrow). Bars, (A) 5 µm; (B-I) 10 µm.
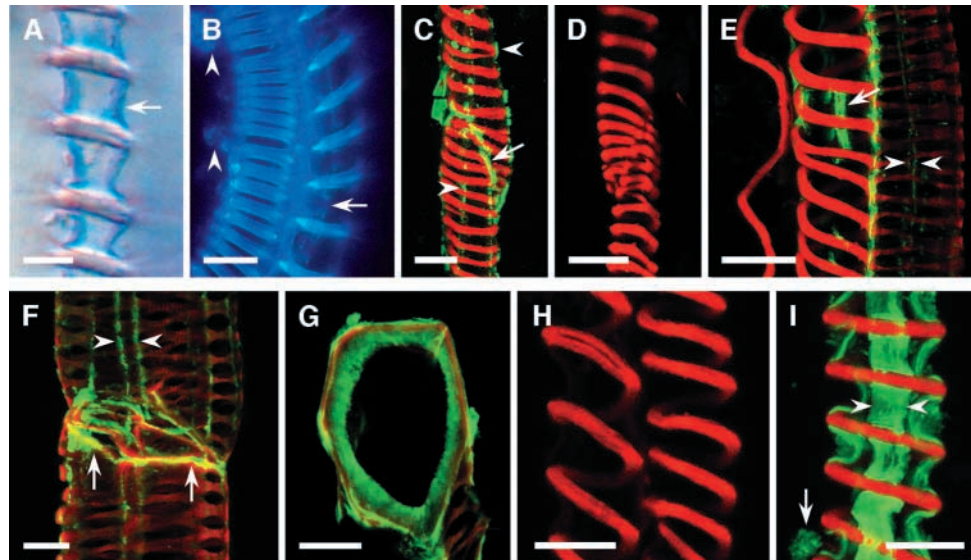
Structure of novel GRP1.8-related proteins

In order to provide a general description of this novel family of GRP1.8-related proteins, all the 20 proteins described above were compared with the amino acid sequence of GRP1.8. This revealed a considerable variation in size, ranging from 73 residues in the barley Hv BG417416 protein to 465 residues for the bean GRP1.8 protein. Variation in size was mainly due to a different number of glycine-rich sequence motifs. The proteins contained a high proportion of both glycine residues, from 41% (Ta BJ286479) to 62% (GRP1.8), and tyrosine (Table 3). Because isolated PX contained a high proportion of serine residues in comparison to GRP1.8, the number of serine residues was also analysed. This revealed a large variation in serine content, ranging from 16.5% for Ta BJ286479 to 1.7% for GRP1.8. This variation was not specific to a plant group because proteins with high and low content of serine residues were present together in the *Arabidopsis* genome (*At AY136328* and *At AB026636*). In order to classify the novel GRP1.8-related proteins, the alignment was limited to the first 40 amino acids of the N-terminal region, excluding the glycine-rich region. Fig. 7A shows the N-terminal part of the amino acid alignment. A phylogenetic tree was generated and the GRP-related proteins could be classified into five main groups (Table 3, Fig. 7B). Groups I and III showed a high proportion of glycine and a low proportion of serine. These groups consisted either of dicotyledonous (group I) or monocotyledonous (group III) species only. Groups II, IV and V showed a

considerable proportion of serine residues. From these studies, we conclude that the mining of databases resulted in many GRP-related proteins which possibly have homologous functions to GRP1.8 in different plant species. The GRP subgroups resulting from this analysis might indicate that we have only started to understand the molecular and biochemical complexity underlying the GRP network in PX.

Discussion

Microscopy of isolated PX

In this paper, a new, clearly distinct structural element containing GRPs is visualized with CLSM in the protoxylem of elongating organs of different plant species belonging to the dicots, monocots and gymnosperms. This structural element is initially deposited in the cell corners along the longitudinal axis of the PX, interconnects the SW and then forms the wall between two dead PX. Finally, a complicated 3D network is deposited containing a large proportion of cell-wall proteins, a unique feature among the cell walls of seed plants. In soybean PX, GRPCWM is stable against detergent extractions, proteinase, pectinase and cellulase hydrolysis, and is closely associated with RG-I, a pectic polysaccharide. It remains to be shown whether GRPs and RG-I form two independent networks or are covalently linked by *O*-glycosylation. The results presented in this paper clearly demonstrate that the cell wall of protoxylem cells is a dynamic and complex structure,

Fig. 6. GRPCWM in the protoxylem of other seed plants. (A-I) Confocal 3D reconstruction of the protoxylem of different species after staining with bean GRP1.8 antibodies. (J) Differential interference contrast, Coomassie-Blue staining. (A) *Arabidopsis thaliana* hypocotyl. The GRP network is restricted to the protoxylem, as in soybean. The ring-shaped SW (arrow) is tilted, probably owing to the collapse of the PX. Arrowheads, helical SW; m, metaxylem. (B) *Nicotiana tabacum* hypocotyl. Two ring-shaped SW are interconnected by a helical SW. (C) *Leucojum vernum*, floral axis. SW in the form of squares, interconnected by four filaments of GRPCWM. (D) *Galanthus nivalis* floral axis. GRPCWM is associated with ring-shaped SW. Arrowheads indicate the position of missing ring-shaped SW. The GRPCWM between two adjacent PX is indicated by arrows. One of the partners was removed by the isolation procedure. (E) *G. nivalis* floral axis. GRPCWM (arrow) interconnects the ring-shaped SW of two PX. Side view of a situation similar to (D). (F) *G. nivalis* floral axis. Rabbit serum control. As in soybean, the GRPCWM is faintly stained with ethidium bromide. (G) *Pinus sylvestris* cotyledon. Thin filaments of GRPCWM interconnect the SW. (H) *Picea abies* hypocotyl. Anastomosing SW are interconnected by GRPCWM. (I) *P. abies* hypocotyl. Rabbit serum control. As shown for other species the GRPCWM is faintly stained with ethidium bromide. (J) *P. abies* hypocotyl. Differential interference contrast microscopy. Arrows, filaments stained with Coomassie Blue. Bars, 10 μm.
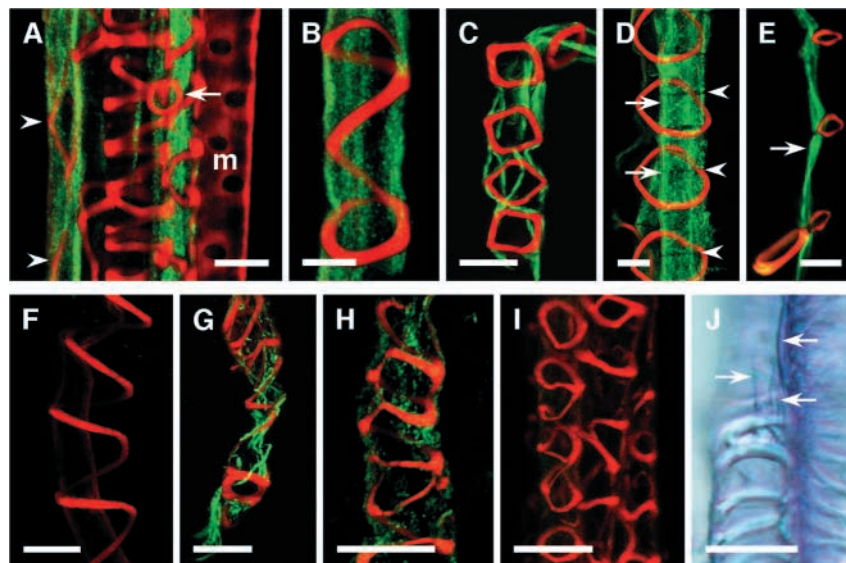
and does not represent only hydrolysed primary walls allowing the stretching of the dead PX, without any further functions.

Isolation of PX

The isolation of fragments of PX showed that the connections between SW and GRPCWM are very resistant to the enzymatic hydrolysis used to soften the tissues and the shearing forces produced by the homogenization. Extraction with SDS or additional hydrolysis with proteinase K, collagenase or cellulase show that GRPCWM is a stable, probably highly cross-linked, structure, being firmly connected with the SW. GRPCWM can therefore be seen as a new material resisting the hydrolases released during the execution of the cell death

Table 3. List of identified GRPs with structures similar to that of bean GRP1.8

| Group	Gene name*	Nucleotide accession	Protein accession	Plant species	References	Residues	G%	Y%	F%	S%
I	Pv X13596/GRP1.8 (g)	X13596	CAA31932	*Phaseolus vulgaris*	Keller et al., 1988	465	62.7	6.8	0.2	1.7
I	Bn Z15045/BNGRP22 (g)	Z15045	CAA78762	*Brassica napus*	Bergeron et al., 1994	291	62.2	4.8	1.0	3.4
I	At AY136328 (g)	AY136328	AAM96994	*Arabidopsis thaliana*	–	255	59.6	4.3	1.1	5.4
I	Pv X13595/GRP1 (g)	X13595	CAA31931	*Phaseolus vulgaris*	Keller et al., 1988	252	58.3	5.1	1.1	4.3
I	Bo BH576806[†] (g)	BH576806	–	*Brassica oleracea*	–	171	52.9	4.6	1.1	5.2
II	Bo BH676349 (g)	BH676349	–	*Brassica oleracea*	–	157	57.9	4.4	2.5	12.7
II	At AB026636 (g)	AB026636	BAA94989	*Arabidopsis thaliana*	–	175	56.5	6.8	1.7	13.1
II	At AB016882 (g)	AB016882	BAB08917	*Arabidopsis thaliana*	–	268	57.0	7.0	1.1	8.9
III	Ta BQ246969 (c)	BQ246969	–	*Triticum aestivum*	–	128	45.3	7.8	2.3	3.9
III	Hv X52580/hvGRP (g)	X52580	CAA36811	*Hordeum vulgare*	Rohde et al., 1990	200	49.0	6.5	1.5	1.5
IV	Hv BG417416 (c)	BG417416	–	*Hordeum vulgare*	–	73	46.5	8.2	0.0	9.5
IV	Ta CA707488[†] (c)	CA707488	–	*Triticum aestivum*	–	68	44.1	7.3	0.0	8.8
V	Sp BG649802[†] (c)	BG649802	–	*Shorghum propinquum*	–	135	57.7	7,4	0.0	9.6
V	Os U40708/GRP 0.9 (g)	U40708	AAA85863	*Oryza sativa*	Fang et al., 1991	183	56.8	8.2	0.0	10.3
V	Os AC024129 (g)	AC024129	–	*Oryza sativa (japonica)*	–	230	50.4	8.2	0.8	13.4
V	Os AAAA01022854 (g)	AAAA01022854	–	*Oryza sativa (indica)*	–	169	50.2	8.2	0.6	12.4
V	Os AP004687 (g)	AP004687	–	*Oryza sativa (japonica)*	–	285	49.4	9.4	1.0	13.3
V	Os AB059239/CAI1 (c)	AB059239	BAB69447	*Oryza sativa (japonica)*	Che et al., 2002	185	49.1	8.1	0.5	14.0
V	Zm BZ726475[†] (g)	BZ726475	–	*Zea mays*	–	248	45.9	3.2	1.6	12.9
V	Zm Y07781/ZmGRP3 (c)	Y07781	CAA69104	*Zea mays*	Goddemeier et al., 1998	256	42.9	3.9	1.1	12.1
V	Ta BJ286479 (c)	BJ286479	–	*Triticum aestivum*	–	200	41.0	5.5	0.5	16.5

*Sequence from genomic DNA (g) or cDNA (c).

[†]Genes partially covered at the 5′ region by isolated clones.

The *GRP* genes are sorted according to the classification developed in Fig. 7B, and according to their percentage of glycine residues. Gene names were given according to the species and the nucleotide accession.

The references refer to the researcher who characterised GRP proteins.
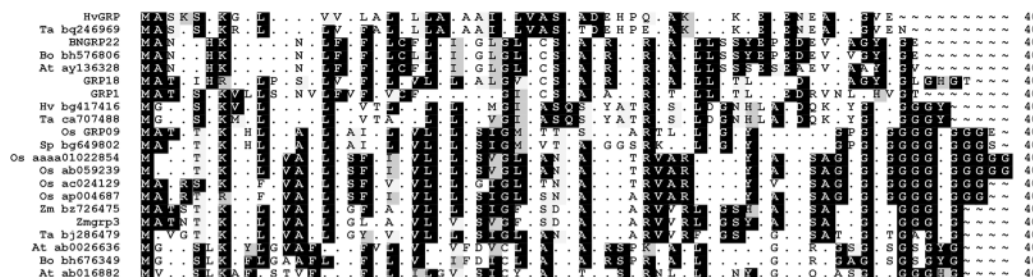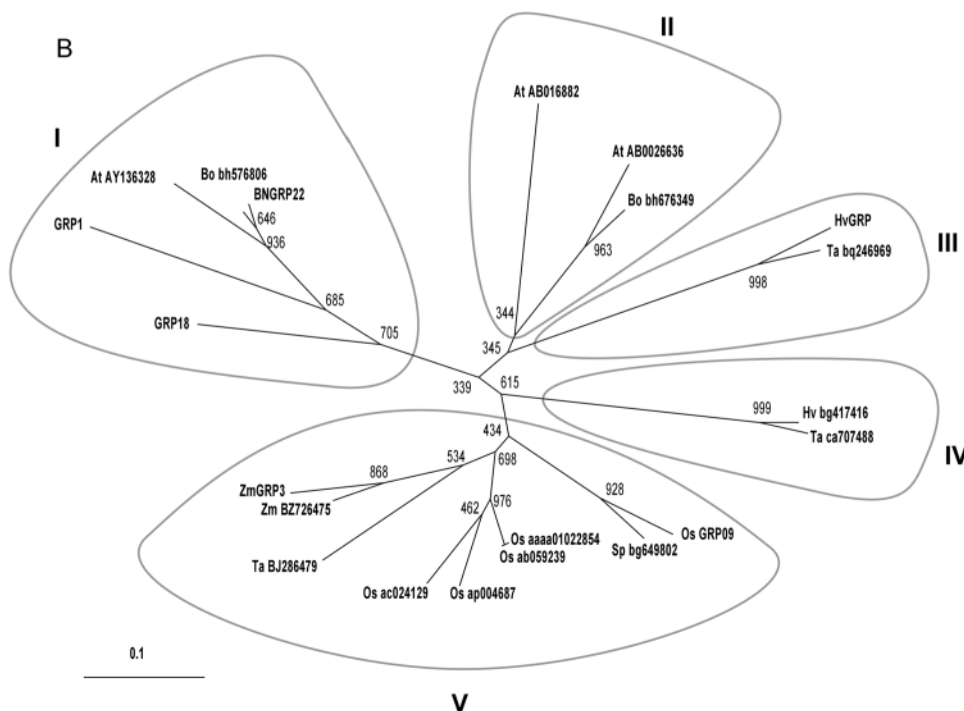
Fig. 7. Analysis of GRP-related sequences from seed plants. (A) Amino acid alignment of the N-terminal region of proteins structurally similar to bean GRP1.8. The first 40 amino acids were used to perform multiple alignments. (B) Classification of plant proteins structurally similar to GRP1.8. The classification was based on multiple protein sequence alignments of the first 40 amino acids of proteins. The bootstrap values for the five main families are indicated at the nodes of the tree. N-terminal amino acid sequences were aligned with PILEUP and analysed with the neighbour-joining method.

program in PX. GRPCWM shares this property with lignified cell walls.

Glycine is enriched in the purified PX fraction by a factor of two to three in comparison to crude cell walls, proving that the bean GRP1.8 antibody recognizes a GRP in the soybean PX. GRP1.8 contains 66% glycine, 9.9% alanine and 7.4% tyrosine (Keller et al., 1988). If the amino acid composition of the soybean homologue is similar and the glycine content of the HRGPs and PRPs is low (as in many representatives), it can be estimated that more than 40% of the amino acids in the PX fraction are associated with GRPs. The remaining amino acids are probably associated with HRGPs and PRPs, proteins associated with lignified cell walls (Bao et al., 1992; Müsel et al., 1997; Ryser et al., 1997; Cassab, 1998). Hydroxyproline is a frequent amino acid in HRGPs and, to a lesser extent, in PRPs and arabinogalactan proteins. It accumulates towards the end of hypocotyl elongation, as already shown for other elongating plant organs (Sadava and Chrispeels, 1973; Cassab, 1998). This observation indicates that hydroxyproline-containing proteins are not essential constituents of GRPCWM. A surprising result of these amino

acid analyses is the high serine content of the isolated PX. Serine is a substrate for *O*-glycosylation in animals, but *O*-glycosylation of serine residues has not yet been demonstrated in plants. A GRP with a content of 68% glycine and 12% serine has been described in the aleurone layer of soybean seeds. The isolated protein also contained 10% monosaccharides (Matsui et al., 1995). The high serine content is worth noting and is similar to the high serine content of the GRPCWM fraction isolated from soybean hypocotyls. It is intriguing that also a class of GRP coding genes with a high serine content was found in the data mining for *GRP1.8*-related genes. It remains to be seen whether the serine-rich GRPs are the main reason for the high serine content in protoxylem walls.

Cytochemistry of GRPCWM

A xyloglucan epitope, recognized by CCRC-M1 antibodies, disappeared already before the initiation of the cell death program from the primary walls of PX (Ryser, 2003). In the present investigation, GRPCWM was not stained with

CCRC-M1. These observations are interesting because the xyloglucans form a network stabilizing the primary walls in the longitudinal axis of the cells (McCann and Roberts, 1991; Carpita and Gibeaut, 1993). A weakening or degradation of this network should facilitate the passive elongation of PX. An intriguing hypothesis is that the GRP network, together with pectins (see below), takes over the function of the xyloglucan network. Such a far-reaching modification of the xyloglucan network still remains to be shown in differentiating PX. It is, however, clear that two different structures are needed to cope with two completely different situations: the highly regulated elongation of living cells and the passive stretching of dead water pipes in the protoxylem.

In ultrathin sections, pectins were localized with JIM5 and JIM7 antibodies in the GRPCWM (Ryser, 2003). The densities of the immunogold label obtained with the two antibodies were similar. However, a decrease in the density of labelling with both antibodies was observed from the apical towards the basal regions of the hypocotyl. With isolated PX, no immunofluorescence was observed with JIM7. JIM5 labelled only the GRPCWM of younger PX, and specific structures at the ends of the tracheary elements. These results indicate that the enzymes used for the preparation of PX preferentially degraded the JIM7 epitope. The decreased JIM5 labelling of older PX is consistent with the results obtained with immunogold labelling mentioned above. Both results might be explained either by a dilution of the pectin or by the increased masking of the pectin epitopes by GRP during the passive elongation of the PX.

The consistent labelling of GRPCWM with CCRC-M2, which recognizes RG-I, was surprising. No signal above background was obtained on ultrathin sections with this antibody. Possible reasons for this difference are a low density of the epitope or masking of the epitope in ultrathin sections by either the embedding medium or cell-wall constituents. The consistent labelling of the GRPCWM with CCRC-M2 indicates that GRP and pectins might be linked together via RG-I. Possible candidates for such links include rhamnose (Willats et al., 2001) and serine, a common *O*-glycosylation site in animals. The observation of stress fibres between SW and the middle lamella of xylem parenchyma cells (Ryser, 2003) indicates that strong links between GRPCWM and pectins of the middle lamellae must exist. In the experiments reported in this paper, a large part of the pectins of the middle lamellae interconnecting the PX and xylem parenchyma cells were hydrolysed by the enzymes used for the isolation of PX.

Structural function of GRPCWM

Preliminary evidence for a structural function of GRP in the development of PX of bean and soybean hypocotyls was obtained already earlier (Keller et al., 1989; Ryser and Keller, 1992; Ryser et al., 1997; Ryser, 2003). Superficially, the GRPCWM resembles the stress fibres of mammalian cells and is attached at well-defined sites on the SW and the middle lamella of xylem parenchyma cells (Ryser, 2003). Occasionally, outward deformations of the SW are observed at places where the SW and the GRPCWM interconnect (U. Ryser et al., unpublished) (Fig. 1E). They are probably a consequence of the stress arising between the dead PX and the elongating xylem parenchyma cells. The final proof for the

structural function of GRPCWM is the insolubility of this structure in boiling SDS and the resistance towards enzymatic hydrolysis and mechanical stress.

GRPs are generally found in seed plants

It is shown in this paper by CLSM that GRPs are widely distributed in seed plants in the modified primary walls of PX and this is corroborated by the finding of *GRP1.8*-related genes in many seed plants. For several reasons, our analysis only revealed a subset of such genes. First, among seed plants, only the *Arabidopsis* and rice genomes are completely sequenced to date. Second, most of the expressed sequence tag information could not be used because these are mostly sequences from the 3′ end of genes, whereas our homology search was dependent on 5′ sequences. Finally, we still do not know in terms of protein sequence what is functionally essential for a GRP in PX. Possibly, only a high content in glycine and some secondary structure motifs are needed, making primary sequence analysis less predictive (Sacchetto-Martins et al., 2000). The newly described class of GRPs with high serine contents is an interesting new type of protein and its cellular and subcellular localization has to be further investigated.

Conclusion

The results presented in this paper demonstrate that the cell wall of protoxylem cells is a complex and dynamic structure. The typical polysaccharide-rich cell wall of living and elongating PX is progressively replaced by the GRP-containing wall of the dead water pipes. An interesting property of these walls is that they apparently can withstand the 'deadly mix' of hydrolases released during the execution of the cell death program in PX. Clear experimental evidence is presented for the first time for the structural function of GRPCWM. Other functions, such as the formation of a hydrophobic surface layer in PX (Ringli et al., 2001b) or a function in the termination of elongation growth remain to be tested experimentally.

References

Altschul, S., Madden, T. L., Schaeffer, A. A., Zhang, J., Zhang, Z., Miller, W. and Lipman, D. J. (1997). Gapped BLAST and PSI-BLAST: a new generation of protein database search programs. *Nucleic Acids Res*. **25**, 3389-3402.

Bao, W., O'Malley, D. M. and Sederoff, R. R. (1992). Wood contains a cell-wall structural protein. *Proc. Natl. Acad. Sci. USA* **89**, 6604-6608.

Bergeron, D., Boivin, R., Baszczynski, C. L. and Bellemare, G. (1994). Root-specific expression of a glycine-rich protein gene in *Brassica napus*. *Plant Sci.* **96**, 87-98.

Carpita, N. C. and Gibeaut, D. M. (1993). Structural models of primary cell walls in flowering plants: consistency of molecular structure with the physical properties of the walls during growth. *Plant J.* **3**, 1-30.

Cassab, G. I. (1998). Plant cell wall proteins. *Annu. Rev. Plant Physiol.* **49**, 281-309.

Che, F. S., Entani, T., Marumoto, T., Taniguchi, M., Takayama, S. and

Isogai, A. (2002). Identification of novel genes differentially expressed in compatible and incompatible interactions between rice and *Pseudomonas avenae*. *Plant Sci.* **162**, 449-458.

Delledonne, M., Xia, Y., Dixon, R. A. and Lamb, C. (1998). Nitric oxide functions as a signal in plant disease resistance. *Nature* **394**, 585-588.

Esau, K. (1977). *Anatomy of Seed Plants.* New York: John Wiley and Sons.

Esau, K. and Charvat, I. (1978). On vessel member differentiation in the bean (*Phaseolus vulgaris* L.). *Ann. Bot.* **42**, 665-677.

Fang, R. X., Pang, Z., Gao, D. M., Mang, K. Q. and Chua, N. H. (1991). cDNA sequence of a virus-inducible, glycine-rich protein gene from rice. *Plant Mol. Biol.* **17**, 1255-1257.

Freshour, G., Clay, R. P., Fuller, M. S., Albersheim, P., Darvill, A. G. and Hahn, M. G. (1996). Developmental and tissue-specific structural alterations of the cell-wall polysaccharides of *Arabidopsis thaliana* roots. *Plant Physiol.* **110**, 1413-1429.

Fry, S. C. (1988). *The Growing Plant Cell Wall: Chemical and Metabolic Analysis.* Harlow, UK: Longman Scientific and Technical.

Fukuda, H. (2000). Programmed cell death of tracheary elements as a paradigm in plants. *Plant Mol. Biol.* **44**, 245-253.

Goddemeier, M. L., Wulff, D. and Feix, G. (1998). Root-specific expression of a *Zea mays* gene encoding a novel glycine-rich protein, ZmGRP3. *Plant Mol. Biol.* **36**, 799-802.

Groover, A., Dewitt, N., Heidel, A. and Jones, A. (1997). Programmed cell death of plant tracheary elements differentiating in vitro. *Protoplasma* **196**, 197-211.

Groover, A. and Jones, A. M. (1999). Tracheary element differentiation uses a novel mechanism coordinating programmed cell death and secondary cell wall synthesis. *Plant Physiol.* **119**, 375-384.

Joseleau, J. P. and Ruel, K. (1997). Study of lignification by noninvasive techniques in growing maize internodes. An investigation by Fourier transform infrared cross-polarization-magic angle spinning ^{13}C-nuclear magnetic resonance spectroscopy and immunocytochemical transmission electron microscopy. *Plant Physiol.* **114**, 1123-1133.

Keller, B., Sauer, N. and Lamb, C. J. (1988). Glycine-rich cell wall proteins in bean: gene structure and association of the protein with the vascular system. *EMBO J.* **7**, 3625-3633.

Keller, B., Templeton, M. D. and Lamb, C. J. (1989). Specific localization of a plant cell wall glycine-rich protein in protoxylem cells of the vascular system. *Proc. Natl. Acad. Sci. USA* **86**, 1529-1533.

Knox, J. P. (1997). The use of antibodies to study the architecture and development of plant cell walls. *Int. Rev. Cytol.* **171**, 79-120.

Lamb, C. and Dixon, R. A. (1997). The oxidative burst in plant disease resistance. *Annu. Rev. Plant Physiol. Plant Mol. Biol.* **48**, 251-275.

Maeda, H. and Ishida, N. (1967). Specificity of binding of hexapyranosyl polysaccharides with fluorescent brightener. *J. Biochem.* **62**, 276-278.

Matsui, M., Toyosawa, I., and Fukuda, M. (1995). Purification and characterization of a glycine-rich protein from the aleurone layer of soybean seeds. *Biosci. Biotechnol. Biochem.* **59**, 2231-2234.

McCann, M. C. and Roberts, K. (1991). Architecture of the primary cell wall. In *The Cytoskeletal Basis of Plant Growth and Form* (ed. C. W. Lloyd), pp. 109-129. London: Academic Press.

Müsel, G., Schindler, T., Bergfeld, R., Ruel, K., Jacquet, G., Lapierre, C., Speth, V. and Schopfer, P. (1997). Structure and distribution of lignin in

primary and secondary cell walls of maize coleoptiles analyzed by chemical and immunological probes. *Planta* **201**, 146-159.

O'Brien, T. P. (1981). The primary xylem. In *Xylem Cell Development* (ed. J. R. Barnett), pp. 14-46. Tunbridge Wells, UK: Castle House Publications.

O'Brien, T. P. and McCully, M. E. (1981). The study of plant structure. Principles and selected methods. Melbourne, Australia: Termacarphi.

Ringli, C., Keller, B. and Ryser, U. (2001a). Glycine-rich proteins as structural components of plant cell walls. *CMLS* **58**, 1430-1441.

Ringli, C., Hauf, G. and Keller, B. (2001b). Hydrophobic interactions of the structural protein GRP1.8 in the cell wall of protoxylem elements. *Plant Physiol.* **125**, 673-682.

Rohde, W., Rosch, K., Kroger, K. and Salamini, F. (1990). Nucleotide sequence of a *Hordeum vulgare* gene encoding a glycine-rich protein with homology to vertebrate cytokeratins. *Plant Mol. Biol.* **14**, 1057-1059.

Ruel, K., Faix, O. and Joseleau, J. P. (1994). New immunogold probes for studying the distribution of the different lignin types during plant cell wall biogenesis. *J. Trace Microprobe Tech.* **12**, 247-265.

Ryser, U. and Keller, B. (1992). Ultrastructural localization of a bean glycine-rich protein in unlignified primary walls of protoxylem cells. *Plant Cell.* **4**, 773-783.

Ryser, U., Schorderet, M., Zhao, G. F., Studer, D., Ruel, K., Hauf, G. and Keller, B. (1997). Structural cell-wall proteins in protoxylem development: evidence for a repair process mediated by a glycine-rich protein. *Plant J.* **12**, 97-111.

Ryser, U. (2003). Protoxylem: the deposition of a network containing glycine-rich cell wall proteins starts in the cell corners in close association with the pectins of the middle lamella. *Planta* **216**, 854-864.

Sachetto-Martins, G., Franco, L. O. and DeOliveira, D. E. (2000). Plant glycine-rich proteins: a family or just proteins with a common motif? *Biochim. Biophys. Acta* **1492**, 1-14.

Sadava, D. and Chrispeels, M. J. (1973). Hydroxyproline-rich cell wall protein (extensin): role in the cessation of elongation in excised pea epicotyls. *Dev. Biol.* **30**, 49-55.

Thompson, J. D., Higgins, D. G. and Gibson, T. J. (1994). CLUSTAL W: improving the sensitivity of progressive multiple sequence alignment through sequence weighting, position-specific gap penalties and weight matrix choice. *Nucleic Acids Res.* **22**, 4673-4680.

Willats, W. G. T., Limberg, G., Buchholt, H. C., Van Alebeek, G. J., Benen, J., Christensen, T., Visser, J., Voragen, A, Mikkelsen, J. D. and Knox, J. P. (2000). Analysis of pectin structure part 2 – analysis of pectic epitopes recognised by hybridoma and phage display monoclonal antibodies using defined oligosaccharides, polysaccharides, and enzymatic degradation. *Carbohydrate Res.* **327**, 309-320.

Willats, W. G. T., McCartney, L., Mackie, W. and Knox, J. P. (2001). Pectin: cell biology and prospects for functional analysis. *Plant Mol. Biol.* **47**, 9-27.

Wood, P. J., Fulcher, R. G. and Stone, B. A. (1983). Studies on the specificity of interaction of cereal cell wall components with Congo red and Calcofluor. Specific detection and histochemistry of (1,3),(1,4)-β-D-glucan. *J. Cereal Sci.* **1**, 95-110.

Zablackis, E., Huang, J., Muller, B., Darvill, A. G and Albersheim, P. (1995). Characterization of the cell-wall polysaccharides of *Arabidopsis thaliana* leaves. *Plant Physiol.* **107**, 1129-1138.